https://doi.org/10.1109/JSTQE.2018.2806084

Reflectivity of superimposed Bragg gratings induced by longitudinal mode instabilities in fiber lasers

Pavel Peterka, Pavel Koška, and Jiří Čtyroký, *Senior Member, IEEE*

***Abstract*—We report on reflectivity of transient Bragg gratings created in the active medium of a fiber laser with longitudinal mode instability. Despite the long history of laser physics, reflectivities of such gratings were theoretically studied and experimentally measured only recently. Based on the coupled-mode theory, we derived a theoretical model of superimposed Bragg gratings for a special case of mode instability known as spontaneous laser line sweeping (SLLS). SLLS fiber lasers exhibit a periodic wavelength drift over an interval of several nanometers, followed by a quick bounce backward, narrowband and mostly single-frequency operation as well as pulsed output with pulse lengths on the order of microseconds. The refractive index modulation inside the active fiber is given by the Kramers-Kronig relations. For ytterbium, the refractive index change in the 1060-nanometer band is directly proportional to the metastable level population with a factor of 2.1×10^{-31} m^3. Taking into account realistic values of temporal damping of the gratings, significant reflectivity on the order of units to tens of percent is estimated. The reflectivity can be controlled by setting the SLLS laser parameters. Effect of the resonator length is shown as an example.**

***Index Terms*—narrow-linewidth lasers, single-frequency lasers, wavelength tunable lasers, mode instability, fiber lasers, fiber Bragg gratings**

I. Introduction

Fiber lasers are considered one of the most rapidly developing branch of lasers [1], but despite their coming to maturity, a number of material and fiber design still remain to be solved. These issues involve, among others, mitigation of limiting effects of stimulated Raman and Brillouin scattering [2, 3], cooling capabilities of the active fibers [4], nonradiative quenching of excited ions [5], low-effective pump absorption [6], photodarkening [7], and instabilities of fiber laser devices [8]. Mitigation of various types of instabilities is currently at the top of research interest in fiber lasers since the transverse mode instability seriously limits maximum output power of single-transverse-mode fiber laser devices [9-11]. Another particularly frequent and dangerous instability is the self-Q-switched pulse mode, which is characterized by intense sub-microsecond pulses with a more or less chaotic repetition rates [12].

One of the recently observed pulse instabilities is the spontaneous or self-induced laser line sweeping (SLLS). The designation of the effect reflects the fact that the self-pulsing is accompanied by a spectacular drift of the laser wavelength, either from shorter towards longer wavelengths followed by an immediate bounce back, as observed in first experiments with ytterbium fiber lasers [13-16], or in the reverse direction, as observed later [17-20]. Self-sweeping ranges up to 20 nm were reported [21]. The self-sweeping regime was observed in fiber lasers with various active fibers, including ytterbium [13-16], erbium [17, 18], thulium [22] bismuth [23] and holmium fibers [24]. SLLS applications in spectral testing of components with narrow spectral features [21] and in testing high-speed spectrum analyzers [25] were demonstrated. A relatively high power, simple design and inherently narrow linewidths make these swept sources attractive for applications in the interrogation of fiber laser arrays and in laser spectroscopy. Thanks to the stable periodic sweeping, SLLS lasers can advantageously serve as a research platform for the investigation of longitudinal mode instabilities in general [26].

The self-sweeping of the laser wavelength can be explained by spatial hole burning along the active fiber. At the threshold, the laser may radiate at a single longitudinal mode which creates a standing wave in the cavity. The population inversion is less depleted at nodes, where the laser intensity is low, than at anti-nodes of the standing-wave, where the laser intensity is high. Therefore, the initially lasing longitudinal mode quickly becomes less preferred than the neighboring longitudinal modes as its gain decreased. The laser wavelength hops to the next longitudinal mode and the situation repeats as long as the spectral gain exceeds the cavity losses. Then the longitudinal mode jumps back to approximately the position of the initial laser wavelength. The SLLS can be recognized as a special case of longitudinal mode instability, where lasing of each longitudinal mode occurs only for a limited time, and lasing of the modes obeys the order of

Manuscript received July 31, 2017. This work was supported by the Czech Science Foundation (16-13306S).
Pavel Peterka and Jiří Čtyroký are with the Institute of Photonics and Electronics of the CAS, Chaberská 57, 18251 Prague, Czech Republic (email: peterka@ufe.cz). Pavel Koška is now with Infineon Technologies Austria AG.
Color versions of one or more of the figures in this letter are available online at http://ieeexplore.ieee.org.
Digital Object Identifier 10.xxx/JSTQE.2018.xxx

https://doi.org/10.1109/JSTQE.2018.2806084

consequential mode hopping. On the other hand, the wavelength sweeping is quasi-continuous because of the mode-hopping nature of the SLLS effect. Since each longitudinal mode radiates for a limited time only, it does not reach the continuous wave regime and emits only in its temporal stage of relaxation oscillations. Therefore, the temporal output of SLLS fiber laser is a pulse train of sustained relaxation oscillations. The narrowband feature of the SLLS favors the stimulated Brillouin scattering (SBS). With increasing pump power, the SLLS regime may often turn into a self-Q-switched regime. It is the longitudinal mode instability that can trigger the self-Q-switched regime, either through the SBS or due to enhanced Q-factor of the cavity by creating highly reflective fiber Bragg gratings (FBGs) that are the subject of this paper.

The FBGs in the active medium of the laser cavity are created since spatial hole burning causes also weak refractive index modulation [27]. The effect of standing waves on the refractive index along the fiber is known for a long time [28, 29]. It was even used for the creation of the first ever FBG [30], but despite the relatively long history of laser physics, the first evaluation of reflectivity of the FBGs spontaneously created in the active media itself [31-33] as well as the inscription of phase gratings [20] has been reported only very recently. Since the reflectivity is significant in a wavelength range just around the lasing wavelength, it is not easy to measure the reflectivity of these FBGs experimentally. Finally, the reflection of about 5 % of such FBGs was successfully measured in a self-swept Yb fiber laser with a polarization-maintaining fiber cavity laser. For the reflectivity measurement, the probe beam was perpendicularly polarized with respect to the self-swept laser radiation [34].

In this paper we present evaluation of the reflectivity of superimposed transient FBGs using a numerical model of a fiber laser with a refractive-index grating build-up. While the case of a single refractive index grating was examined earlier [32], here we present a more realistic case of several superimposed gratings with damped modulation depths. A special SLLS case of the longitudinal mode instability is considered because the long-term stable periodic operation of this special case allows easier mathematical formulation of the FBG theoretical model and gives illustrative results. In the second section we describe a theoretical model of transient FBGs in a SLLS fiber laser. A brief summary of the theoretical model for a single grating [32] is followed by detailed derivation of the theoretical model for a series of superimposed gratings. In the third section we present the calculation of refractive index modulation of superimposed gratings and spectra of their reflectivity. We show that despite a small modulation depth, high reflectivity and thus a rapid enhancement of the Q-factor of the cavity can be easily achieved. Differences in reflectivities of the single FBG and multiple superimposed damped FBGs are discussed.

II. Theoretical Model of Transient FBGs in a Self-Swept Fiber Laser

Theoretical modelling of FBGs in a self-swept fiber laser consists of several steps: we begin with the evaluation of the refractive index modulation without interference effects, then we consider the interference pattern, and finally we evaluate the reflectivity of the refractive index gratings. For the sake of brevity and consistency with previous results, we split the description of the theoretical model into two subsections. In the first subsection we briefly summarize the method of refractive index modulation described in [32]. In the second subsection, the novel part of the theoretical model that deals with superimposed fiber Bragg gratings is described in detail.

A. Estimation of the refractive index modulation

We explain the method of estimation of the refractive index modulation on an example of self-swept ytterbium-doped fiber laser [32]. The fiber laser was built in the Fabry-Perot configuration shown in Fig. 1. The Yb-doped fiber was fabricated in house and has the inner hexagonal-shape cladding with an outer diameter of 125 μm. Parameters of the active fiber and the laser cavity are listed in Table I. The combined length of the passive fibers of the signal branches of the 1% tap and the signal and pump combiner was $L_{passive}$ = 3.3 m. The laser operated in the self-sweeping mode within an interval from the laser threshold pump power of 0.4 W to the pump power of about 1.5 W which corresponded to the self-swept laser output power of 0.5 W. Starting from about 0.4 W of the output power, the self-sweeping became less regular. As an example, at the 0.4 W of the output, the Yb fiber laser swept around 1062 nm in an interval of 2.6 nm with a sweeping rate of 1.5 nm/s and period of the pulse train T = 29 μs.

Considering the parameters of the Yb-fiber laser listed above and the input pump power of 1 W that correspond to the laser output of about 0.4 W, we calculated the longitudinal evolution of the pump and laser signal powers P^+ and P^- that propagate in forward and backward directions, respectively. The optical power distribution along the fiber laser resonator is shown in Fig. 2. The optical power evolution was calculated using a numerical model that solves simultaneously laser rate equations and propagation equations [35, 36]. The model was initially developed for thulium fiber devices but it is easily adaptable to various rare-earth-doped fibers by selecting of the respective spectroscopic parameters. The interference effects were not involved in the calculations yet, in other words, the physical quantities were assumed constant (averaged) over fiber section Δz, while it holds $L_{YDF} >> \Delta z >> \Lambda_0$, where Λ_0 is the pitch of the grating induced by the standing wave of the single-longitudinal mode of the laser cavity. Grating pitch Λ_0 = 0.36 μm corresponds to the laser wavelength of 1062 nm.

The interference pattern inside the single-frequency laser is governed by the interference equation and the optical power oscillates between the maxima and minima given by $P_{max/min} = P^+ + P^- \pm 2 (P^+ P^-)^{1/2}$. The visibility of interference fringes depends on the ratios of the forward and backward laser signal powers and maximum visibility appears at the position where both waves have the same power, see the black curve in Fig. 2. The population of the upper laser level can be derived from the laser rate equations [36] as:

$$N_2 = \frac{N_{tot} W_a}{W_a + W_e + 1/\tau}, \quad W_{a(e)} = \int \frac{\Gamma P \sigma_{a(e)}}{h\nu A} \mathrm{d}\nu, \qquad (1)$$

https://doi.org/10.1109/JSTQE.2018.2806084

$$\Gamma = \iint_{core} \mathbf{e}^{T}(x,y)\cdot\mathbf{e}^{T*}(x,y)dx\,dy \qquad (2)$$

where τ is the excited level lifetime, W_a and W_e are the absorption and emission rates, $h\nu$ is the photon energy, A is the core area, σ_a and σ_e are the Yb absorption and emission cross sections, and P is the total optical power at a given longitudinal position and frequency ν, respectively. Γ is the overlap factor representing the fraction of the fundamental-transverse mode power interacting with dopants [35]. Assuming that ytterbium ions are homogenously distributed in the core, the overlap factor is given by eq. (2). The transverse distribution of the electric field of the fundamental transverse mode is described by $\mathbf{e}^T(x, y)$ normalized so that the integral of its squared absolute value over the fiber cross section is unity.

TABLE I
PARAMETERS USED IN THE MODEL OF THE SELF-SWEPT FIBER LASER

Parameter	Symbol	Value
Yb ions concentration	N_{tot}	4.63×10^{26} m^{-3}
fiber core diameter	$2a$	5 µm
numerical aperture	NA	0.18
Yb fiber length	L_{YDF}	10 m
Overall cavity length	$L_{YDF+}\,L_{passive}$	13.3 m
excited level lifetime	τ	1.5 ms
pump wavelength	λ_p	977 nm
mean signal wavelength	λ_s	1062 nm
background loss in the core	α_{BG}	0.4 dB/m
overall pump absorption	α_p	9.3 dB
pump overlap	Γ_p	0.356×10^{-3}
signal overlap	Γ	0.87
insertion loss of the combiner	$IL_{combiner}$	0.46 dB
pump absorption cross section	$\sigma_a(\lambda_p)$	13.0×10^{25} m^2
pump emission cross section	$\sigma_e(\lambda_p)$	12.8×10^{25} m^2
signal absorption cross section	$\sigma_a(\lambda_s)$	0.023×10^{25} m^2
signal emission cross section	$\sigma_e(\lambda_s)$	1.78×10^{25} m^2

The refractive index change is related to the excited level population through the Kramers-Kronig relation. Since for Yb the dominant contribution comes from the UV transition, the refractive index change is almost spectrally independent in the wavelength range of the Yb fiber laser [28, 29, 32]. The refractive index change around 1062 nm is then proportional to the metastable level population N_2 via relation [32]:

$$\Delta n = \xi N_2, \quad \xi = 2.1\times10^{-31}\ \mathrm{m}^3 \qquad (3)$$

The resulted refractive index modulation for the case of single grating is represented by the black curve in Fig. 3. Note that only the envelope of the refractive index modulation can be seen from the figure because the grating pitch is seven orders of magnitude shorter than the fiber length.

B. Reflectivity of the transient Bragg grating

The calculation of reflectivity of superimposed FBGs is based on the coupled-mode theory [37-39] applied to the case of fiber gratings [40-42]. Since the superimposed transient FBGs that are generated in the self-swept fiber lasers are of a rather unique type, we have to modify the derivation of equations governing the gratings' reflectivity. We do not provide complete derivation as it is based on the coupled-mode theory detailed in numerous references. Instead, we outline the derivation of modifications specific to our particular grating´s case, as shown below. We follow mostly the notation used in the book by Othonos and Kalli [40].

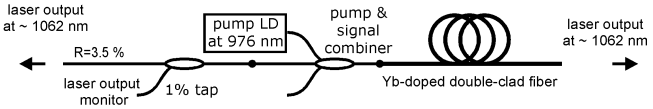

Fig. 1. Experimental setup of the self-swept ytterbium fiber laser.

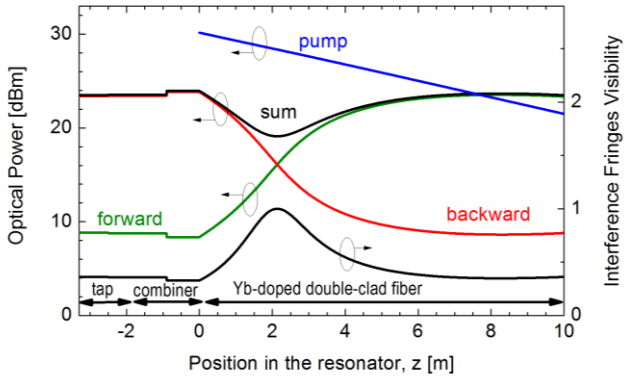

Fig. 2. Longitudinal evolution of the optical power of the pump and laser signal inside the cavity. Note that the position z = 0 is arbitrarily chosen at the beginning of the Yb-doped fiber. The visibility of the interference fringes of the standing wave is largest at the position where the backward and forward waves have equal amplitudes.

Given that only the fundamental mode is excited, we can write the transverse component of the electric field in the single-mode optical fiber as a superposition of the forward and backward propagating waves, comp. equation (5.3) in Othonos and Kalli [40]:

$$\mathbf{E}^T(x,y,z,t) = \left[a(z)\,\mathrm{e}^{i\beta z} + b(z)\,\mathrm{e}^{-i\beta z}\right]\mathbf{e}^T(x,y)\,\mathrm{e}^{-i\omega t}, \qquad (4)$$

where the coefficients $a(z)$ and $b(z)$ are slowly varying amplitudes of the fundamental mode propagating in the forward and backward directions, respectively. The propagation constant β is given by $2\pi\, n_{eff}/\lambda$. In the presence of a periodic perturbation of the refractive index profile with the spatial period Λ_0 along the fiber, the forward and backward modes are coupled via the following set of differential equations, comp. equations (5.4) and (5.5) in [40]:

$$\frac{da}{dz} = iaC + ibC\,\mathrm{e}^{-i2i\beta z}$$
$$\frac{db}{dz} = -ibC - iaC\,\mathrm{e}^{2i\beta z} \qquad (5)$$

Generally, couplings between various modes have to be considered and described by the respective coupling coefficients. In our particular case of single-mode propagation, the coupling is described by a single coupling coefficient C [37, 40]:

$$C(z) = \frac{\omega}{4n_{co}c_0}\iint_{\infty}\Delta\varepsilon(x,y,z)\,\mathbf{e}^T(x,y)\cdot\mathbf{e}^{T*}(x,y)dx\,dy, \qquad (6)$$

where $\Delta\varepsilon(x,y,z)$ is the relative permittivity perturbation which is approximately equal to $2n_{co}\Delta n$ for the perturbation

https://doi.org/10.1109/JSTQE.2018.2806084

$\Delta n \ll n_{co}$. Note that the normalization factor $1/(n_{co}c_0)$ in eq. (6) appears due to the normalization of the transversal electric field $\mathbf{e}^T(x, y)$ defined in section III.A; c_0 is the vacuum speed of light. Since we assume homogeneous ytterbium doping in a relatively small core (it is not a large-mode-area fiber), we correspondingly also assume that the refractive index changes occur only in the core and are almost uniform. Then, the coupling coefficient C is given by:

$$C = \sigma + 2\kappa\cos\left(\frac{2\pi}{\Lambda_0}z + \varphi(z)\right), \tag{7}$$

where

$$\sigma = \frac{\omega}{2c_0}\Delta n_{DC}(z)\Gamma, \tag{8}$$

and

$$\kappa = \frac{\omega}{4c_0}\Delta n_{AC}(z)\Gamma. \tag{9}$$

The coupling coefficient C is given by the sum of the slowly varying "DC" coupling coefficient σ given by the period-averaged refractive index modulation Δn_{DC}; and the fast varying "AC" part characterized by the "AC" coupling coefficient κ given by the refractive index modulation depth Δn_{AC}. In our case of single-frequency operation of the fiber laser, we may assume that Δn_{AC} can vary along the fiber grating without any phase shift, i. e., $\varphi(z) = 0$. The effective index n_{eff} of the fundamental mode is approximated by n_{co} in the definition of σ. The angular frequency $\omega = 2\pi c_0/\lambda_0$ is evaluated at the wavelength λ_0 where the self-sweeping starts. Under the so-called "synchronous approximation" [38, 42], which neglects terms rapidly oscillating in z, we can write equations (5) by using the coupling coefficients σ and κ as follows:

$$\begin{aligned}\frac{da}{dz} &= ia\sigma + ib\kappa\, e^{-i2z(\beta-\pi/\Lambda_0)}\\ \frac{db}{dz} &= -ib\sigma - ia\kappa^*\, e^{i2z(\beta-\pi/\Lambda_0)}\end{aligned} \tag{10}$$

So far, the single period of the refractive index modulation Λ_0 was assumed. However, in the self-swept fiber laser, each lasing longitudinal mode m inscribes its own transient grating with the spatial period Λ_m:

$$\Lambda_m = \frac{\lambda_m}{2n_{eff,m}} \approx \frac{\lambda_0 + m\Delta\lambda}{2n_{eff,0}} = \frac{\lambda_0}{2_{eff,0}} + \frac{m}{L}\left(\frac{\lambda_0}{2n_{eff,0}}\right)^2, \tag{11}$$

where $n_{eff,m}$ is the effective index of the fundamental transverse mode of the m-th longitudinal mode where the index m is relative to the initial lasing longitudinal mode for which m=0. The characteristic lifetime of the transient gratings is assumed to be comparable to the inversion population build-up [43]:

$$t_{sat} = \frac{\tau}{1 + \frac{P_p}{P_p^{sat}} + \frac{P_s}{P_s^{sat}}}. \tag{12}$$

For the fiber laser parameters and optical powers used for the calculation of Fig. 2, we got t_{sat} of around 100 μs and the ratio T/t_{sat} = 0.29, where T is the period of the pulse train of the sustained relaxation oscillations. While for the slow refractive index change Δn_{DC} we can assume negligible changes within the time scale comparable to t_{sat}, the fast refractive index change Δn_{AC} may vary considerably within such a time scale. Let us denote the estimates of the refractive index modulations obtained from the steady state numerical model by Δn_{AC0} and Δn_{DC0}. Then we estimate the overall refractive index modulation Δn as a series of damped refractive index gratings with spatial periods Λ_m:

$$\Delta n(z) = \Delta n_{DC0}(z) + \sum_{m=1}^{N_{mod}} D(z)\exp\left(-\frac{(m-1)T}{\tau_{FBG}}\right)\cos\left(\frac{2\pi}{\Lambda_{m-1}}z\right), \tag{13}$$

where N_{mod} is the number of longitudinal modes involved, and m denotes the index of the respective longitudinal mode. The characteristic lifetime τ_{FBG} is comparable to t_{sat}; however, it is not known because the numerical model of the laser assumes steady state, i. e., the model is not time-resolved. Therefore, the ratio T/τ_{FBG} is a parameter that we will vary in the following calculations of the FBG reflectivities. The fast refractive index modulation of the superimposed transient grating is represented by the second term on the right-hand side of eq. (13) and its envelope is $\Delta n_{AC}(z)$. The coefficient D of the series above is set in such a way that the envelope $\Delta n_{AC}(z)$ never exceeds the fast refractive index modulation $\Delta n_{AC0}(z)$:

$$D(z) = \frac{\Delta n_{AC0}(z)}{\sum_{m=1}^{N_{mod}} e^{-\frac{(m-1)T}{\tau_{FBG}}}} \tag{14}$$

In the case of the series of gratings with close periods Λ_m, the coupled-mode equations (10) can be transformed into the following equations:

$$\begin{aligned}\frac{da}{dz} &= ia\sigma + ib\kappa\, e^{-i2z\beta}\sum_{m=1}^{N_{mod}} De^{-\frac{(m-1)T}{\tau_{FBG}}} e^{iK_{m-1}z}\\ &= ia\sigma + ib\kappa D\, e^{-i2z\beta + iK_0 z}\left(1 + \sum_{m=1}^{N_{mod}-1} e^{-\frac{mT}{\tau_{FBG}}} e^{i(K_m - K_0)z}\right),\end{aligned} \tag{15}$$

$$\frac{db}{dz} = -i\sigma b - ia\kappa^*\, e^{i2z\beta}\sum_{m=1}^{N_{mod}} De^{-\frac{(m-1)T}{\tau_{FBG}}} e^{-iK_{m-1}z}, \tag{16}$$

$$K_m = \frac{2\pi}{\Lambda_m} \tag{17}$$

Note that the first term in the summations containing K_0 can be separated from the sum as shown in eq. (15). Equations (15) and (16) can be simplified by introducing a new form of slowly varying amplitudes $A=a\exp(i\delta z)$ and $B=b\exp(-i\delta z)$, where $\delta = \beta - \pi/\Lambda_0$. Equations (15) and (16) now read as follows:

$$\frac{dA}{dz} = i(\sigma + \delta)B + i\kappa D\, B\left(1 + \sum_{m=1}^{N_{mod}-1} e^{-\frac{mT}{\tau_{FBG}}} e^{i(K_m - K_0)z}\right) \tag{18}$$

$$\frac{dB}{dz} = -i(\sigma + \delta)B - i\kappa^* D\, A\left(1 + \sum_{m=1}^{N_{mod}-1} e^{-\frac{mT}{\tau_{FBG}}} e^{-i(K_m - K_0)z}\right). \tag{19}$$

https://doi.org/10.1109/JSTQE.2018.2806084

From equations (16) and (17) we can obtain the Riccati differential equation for the ratios of amplitudes of backward and forward propagating modes $R(z)=B(z)/A(z)$:

$$\frac{dR}{dz} = -i\kappa^* D\left(1+\sum_{m=1}^{N_{\mathrm{mod}}-1} \mathrm{e}^{-\frac{mT}{\tau_{FBG}}} \mathrm{e}^{-i(K_m-K_0)z}\right) - \\ -i2(\delta+\sigma)R - i\kappa D\left(1+\sum_{m=1}^{N_{\mathrm{mod}}-1} \mathrm{e}^{-\frac{mT}{\tau_{FBG}}} \mathrm{e}^{i(K_m-K_0)z}\right)R^2. \quad (20)$$

Since the coupling coefficients vary along the active fiber, the Riccati equation (20) has to be solved numerically, e. g., by the Runge-Kutta method. The initial condition for the numerical solution is that the amplitude of the backward wave at the end of the grating is zero, $R(z = L) = 0$. The value of the optical power reflectivity is then given by $|R|^2$. The validity of the model was checked on the known case of a single FBG by using the transfer matrix method [42] and examples described therein.

III. Results and Discussion

A. Effect of the ratio T/τ_{FBG}

Firstly, we analyzed the refractive index grating build-up and its optical power reflectivity for the case that is as much similar as possible to the experimental self-swept fiber laser in Fig. 1. The refractive index modulation along the active fiber calculated according to (13) is shown in Fig. 3a. The simplified scheme of the laser setup is shown in the inset for convenience. Since the ratio T/τ_{FBG} could not be obtained from the model described in section III.A, we calculated the gratings for several values T/τ_{FBG} around the value T/t_{sat}=0.29. The value T/τ_{FBG} =10 represents a case when the grating inscribed by a single longitudinal mode dominates. Indeed, the modulation depth of the second grating is e^{-10} times smaller than the modulation depth of the grating created by the initial longitudinal mode. In this limiting case, almost complete reflection can be expected. For the more realistic case of superimposed gratings, the maximum reflectivity decreases to 55, 9.1, 1.2, and 0.04 % for the T/τ_{FBG} ratio of 1, 0.29, 0.1 and 0.01, respectively. The decrease of reflectivity can be explained from the Fig 3a. The more gratings are superimposed on each other, the narrower the apodization of the refractive index modulation is, i. e., the shorter the FBG is, while the modulation depth is not changed. Therefore, the reflectivity decreases for slower temporal damping of the gratings.

B. Effect of the resonator length

In the previous section we have seen that the refractive index grating becomes shorter for slower temporal damping of the individual gratings, *i. e.*, a larger number of gratings are effectively involved in the superposition. The peak of the refractive index modulation depends not only on the power ratio of the forward and backward waves in the laser cavity but also on the interference pattern of the electric field of the forward and backward waves. It means that the peak may shift along the active fiber for different lengths of the resonator. Indeed, the shift of the phase grating pattern for different resonator lengths was also observed experimentally [20]. The refractive index modulation pattern for a laser resonator created only from the active fiber itself is shown in Fig. 4(a). For the sake of the comparison of the two cases, only the length of the passive part was changed and the other parameters remained unchanged. The length of the resonator determines the position of the interferogram local maxima. The maximum reflectivity decreases to 75, 33, 7.9, and 0.36 % for the T/τ_{FBG} ratio of 1, 0.29, 0.1 and 0.01, respectively. It was experimentally demonstrated that the self-sweeping regime can be to some extent controlled by changing the pump wavelength [17, 19] or the resonator length [20]. The results presented in this paper indicate that the control of the self-sweeping regime can be accomplished not only by changes in the spectral gain [14, 19] or phase grating [20] but also by a change in the reflectivity of the transient refractive index gratings.

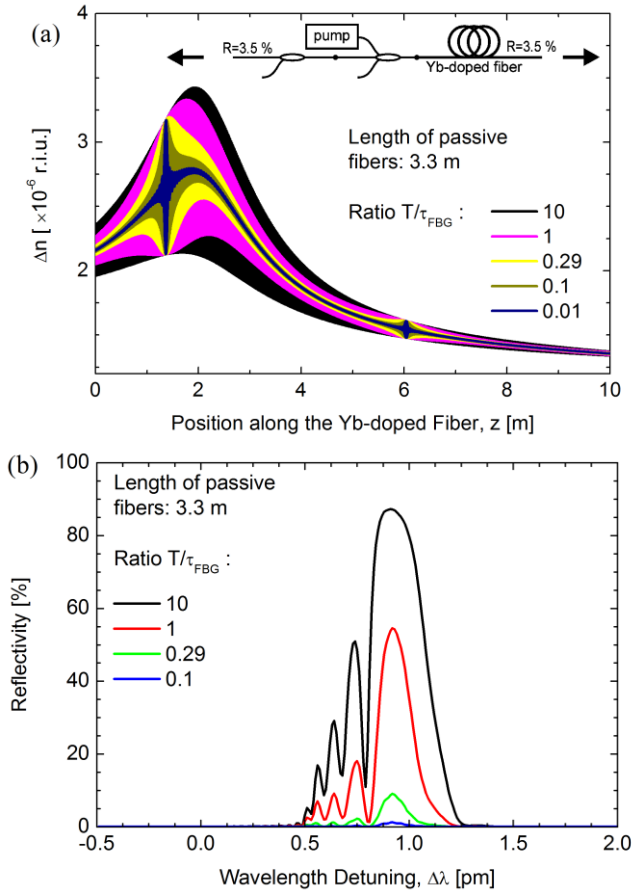

Fig. 3. (a) Refractive index modulation along the active fiber for various values of T/τ_{FBG}. The value T/τ_{FBG}=10 corresponds to practically only one grating (the gratings are not superimposed on each other). The value T/τ_{FBG} = 0.29 corresponds to the case of $\tau_{FBG} = t_{sat}$. The scheme of the self-swept fiber laser of the numerical model is in the inset. (b) Reflectivity of transient fiber Bragg gratings created by the standing waves of the consequential hopping longitudinal modes for various values of T/τ_{FBG}.

It should be recalled that we made use of several relevant approximations in this paper. Firstly, sinusoidal refractive index modulation is assumed, but in fact, the modulation can be different as shown for an analogical case of spatial hole burning in the erbium-doped twin-core fiber [44]. Secondly, the steady-state model is assumed and the change in the refractive index is compared with the unpumped state. In this case, the refractive index change is always positive and accordingly, the red-shift wavelength detuning of the maximum FBG reflectivity is obtained. On the other hand, the local change in the refractive index along the fiber can

https://doi.org/10.1109/JSTQE.2018.2806084

be also negative during the actual laser operation and correspondingly, the blue-shift wavelength detuning of the maximum FBG reflectivity can be obtained. The temporally resolved model, yet with the spatial step >> Λ_0, would be the natural upcoming extension of the model presented in this paper. Such a model shall allow description of the blue-shift wavelength detuning of the FBG reflection peak. However, the potential non-sinusoidal refractive index modulation can be simulated only with a spatially resolved model that resolves spatial features on the scale << Λ_0, which is a extremely demanding from the point of view of programming as well as computing time. Indeed, in the case of the erbium-doped twin-core fiber [44] the grating pitch was on the order of millimeters, but the pitch of the transient FBG is three orders of magnitude shorter and the computing time will be correspondingly longer. Fortunately, the simulations can be compared with measurements at least qualitatively, because first experimental evidence of reflectivity of the transient FBGs appeared in a conference paper recently [34]. More details about the experiment were revealed later in a journal paper [45] while our paper was under reviewing. The self-swept fiber laser examined in [45] was principally similar to the setup described here. The measured reflectivity of the FBG was about 7 %, the bandwidth was 50 MHz (0.2 pm) and a number of small sidelobes in the short-wavelength side of the reflection peak were observed. All these features correspond qualitatively to the reflection spectra calculated above by our model despite various approximations used in the model.

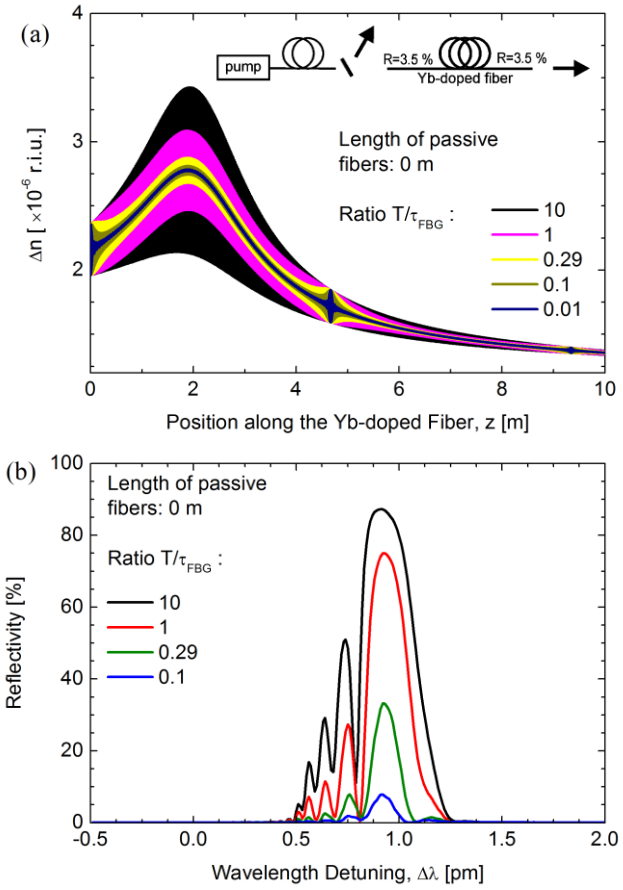

Fig. 4. (a) Refractive index modulation along the active fiber for various values of T/τ_{FBG} and for fiber laser without any passive fiber. (b) Reflectivity of transient fiber Bragg gratings created by the standing waves of consequentially hopping longitudinal modes for various values of T/τ_{FBG}.

IV. Conclusions

We presented evaluation of the reflectivity of the Bragg gratings that are spontaneously built-up in fiber lasers with longitudinal mode instabilities. The FBG reflectivities were reported in self-swept fiber lasers which represent a unique case of longitudinal-mode-instability lasers. We described a significantly improved theoretical model of transient FBG in a self-swept fiber laser by taking into account a superimposition of many gratings created by lasing longitudinal modes which are consecutively hopping in the direction of decreasing or increasing frequencies. Detailed derivation of the theoretical model is presented. The model is based on the coupled-mode theory and takes the advantage of close proximity of periods of the superimposed gratings, which corresponds to close frequency spacing of the respective longitudinal modes responsible for the individual grating build-ups. The resulted spectra of FBG reflectivity show that the overall reflectivity of the series of superimposed gratings decreases but for realistic values of temporal damping of the transient gratings they can still reach significant values on the orders of units or tens of percent. The reflectivity depends on the mutual position of the interference pattern and in the ratio of the optical power of the forward and backward propagating laser signal. Therefore, the reflectivity can be to some extent controlled by parameters of the laser. We have shown the influence of the resonator length. The calculated reflection spectra correspond qualitatively to the recently reported reflectivity measurement of spontaneously created distributed Bragg mirror in a fiber laser with a similar setup.

The model represents an important step towards the understanding of origins of the self-sweeping of fiber lasers, namely the direction of sweeping – blue shift or red shift, and consequently it will allow for control the self-sweeping operation and design of self-swept laser for specific application. Therefore, the model is important from the point of view of practical applications as well as laser physics. The range of practical applications of swept laser sources is increasing and the self-swept fiber lasers may be useful wherever high power and cost-effectiveness are important and the slow scanning speed is not a big obstacle, e. g., in the interrogation of fiber sensor arrays, precise laser spectroscopy, hyperspectral component testing, Brillouin optical spectrum analyzers, etc. Since the self-sweeping is a special case of mode instabilities, the results will be beneficial for the investigation of longitudinal mode instabilities in general and their mitigation. In turn, the understanding of triggering the self-Q-switched regimes may result in the development of cost-effective, high-power self-Q-switched fiber laser. Despite fundamental differences between the transversal and longitudinal mode instabilities, both types of instabilities are analogical in terms of creating the refractive index grating along the fiber. Therefore, the knowledge acquired in the description of transient FBG may also be useful for understanding the transversal mode instabilities.

References

[1] M. N. Zervas, and C. A. Codemard, "High Power Fiber Lasers: A Review," *IEEE J. Sel. Top. Quantum Electron.*, vol. 20, no. 5, pp. 219-241, Sept.-Oct. 2014.

https://doi.org/10.1109/JSTQE.2018.2806084

[2] A. Tünnermann, T. Schreiber, and J. Limpert, "Fiber lasers and amplifiers: an ultrafast performance evolution," *Appl. Opt.*, vol. 49, no. 25, F71-F78, July 2010.

[3] K. Schuster, S. Unger, C. Aichele, F. Lindner, S. Grimm, D. Litzkendorf, J. Kobelke, J. Bierlich, K. Wondraczek, and H. Bartelt, "Material and technology trends in fiber optics.," *Adv. Opt. Technol.*, vol. 3, no. 4, pp. 447–468, May 2014.

[4] J. M. O. Daniel, N. Simakov, A. Hemming, W. A. Clarkson, and J. Haub, "Metal clad active fibres for power scaling and thermal management at kW power levels," *Opt. Express*, vol. 24, no. 16, pp. 18592-18606, Aug. 2016.

[5] C. C. Baker, E. J. Friebele, A. A. Burdett, D. L. Rhonehouse, J. Fontana, W. Kim, S. R. Bowman, L. B. Shaw, J. Sanghera, J. Zhang, R. Pattnaik, M. Dubinskii, J. Ballato, C. Kucera, A. Vargas, A. Hemming, N. Simakov, and J. Haub, "Nanoparticle doping for high power fiber lasers at eye-safer wavelengths," *Opt. Express*, vol. 25, no. 12, pp. 13903-13915, June 2017.

[6] P. Koska, P. Peterka and V. Doya, "Numerical modeling of pump absorption in coiled and twisted double-clad fibers," *IEEE J. Sel. Top. Quantum Electron.*, vol. 22, no.2, pp. 55-62, March-April 2016.

[7] J.-F. Lupi, M. Vermillac, W. Blanc, F. Mady, M. Benabdesselam, B. Dussardier, D. R. Neuville, "Impact of cerium and lanthanum on the photo-darkening and photo-bleaching mechanisms in thulium-doped fibre," *Opt. Mat.*, vol. 72, pp. 106-114, Oct. 2017.

[8] D. J. Richardson, J. Nilsson, and W. A. Clarkson, "High power fiber lasers: current status and future perspectives [Invited]," *J. Opt. Soc. Am. B*, vol. 27, no. 11, pp. B63-B92, Nov. 2010.

[9] C. Jauregui, H.-J. Otto, S. Breitkopf, J. Limpert, and A. Tünnermann, "Optimizing high-power Yb-doped fiber amplifier systems in the presence of transverse mode instabilities," *Opt. Express*, vol. 24, no. 8, pp. 7879-7892, Apr. 2016.

[10] Smith, A. V., and Smith, J. J., "Mode instability thresholds for Tm-doped fiber amplifiers pumped at 790 nm," *Opt. Express*, vol. 24, no. 2, pp. 975–992, Jan. 2016.

[11] M. N. Zervas, "Transverse mode instability analysis in fiber amplifiers [Invited]," in *Proc. SPIE 10083*, Fiber Lasers XIV: Technology and Systems, San Francisco, California, USA, Jan 28, 2017, p. 100830M.

[12] A. V. Kir'yanov, Y. O. Barmenkov, and M. V. Andres, "An experimental analysis of self-Q-switching via stimulated Brillouin scattering in an ytterbium doped fiber laser," *Laser Phys. Lett.*, vol. 10, no. 5, p. 055112, May 2013.

[13] A. V. Kir'yanov, and N. Il'ichev, "Self-induced laser line sweeping in an ytterbium fiber laser with non-resonant Fabry-Perot cavity," *Laser Phys. Lett.*, vol. 8, no. 4, pp. 305-312, Apr. 2011.

[14] I. A. Lobach, S. I. Kablukov, E. V. Podivilov, and S. A. Babin, "Broad-range self-sweeping of a narrow-line self-pulsing Yb-doped fiber laser," *Opt. Express*, vol. 19, 17632-17640 (2011).

[15] P. Peterka, P. Navrátil, J. Maria, B. Dussardier, R. Slavík, P. Honzátko, and V. Kubeček, "Self-induced laser line sweeping in double-clad Yb-doped fiber-ring lasers," *Laser Phys. Lett.*, vol. 9, no. 6, pp. 445-450, June 2012.

[16] P. Peterka, J. Maria, B. Dussardier, R. Slavik, P. Honzatko, and V. Kubecek, "Long-period fiber grating as wavelength selective element in double-clad Yb-doped fiber-ring lasers," *Laser Phys. Lett.*, vol. 6, no. 10, pp. 732-736, Oct. 2009.

[17] P. Peterka, P. Navrátil, B. Dussardier, R. Slavík, P. Honzátko, and V. Kubeček, "Self-induced laser line sweeping and self-pulsing in double-clad fiber lasers in Fabry-Perot and unidirectional ring cavities," *In Proc SPIE 8433*, SPIE Photonics Europe, Brussels, Belgium, 16–20 April 2012, p. 843309.

[18] P. Navratil, P. Peterka, P. Vojtisek, I. Kasik, J. Aubrecht, P. Honzatko, and V. Kubecek, "Self-swept erbium fiber laser around 1.56 μm," Opto-Electron. Rev., vol. 26, no. 1, pp. 29-34, March 2018.

[19] P. Navratil, P. Peterka, P. Honzatko, and V. Kubecek, "Reverse spontaneous laser line sweeping in ytterbium fiber laser," *Laser Phys. Lett.*, vol. 14, no. 3, p. 035102, March 2017.

[20] I. A. Lobach, S. I. Kablukov, E. V. Podivilov, and S. A. Babin, "Self-scanned single-frequency operation of a fiber laser driven by a self-induced phase grating," *Laser Phys. Lett.*, vol. 11, no. 4, p. 045103, Apr. 2014.

[21] I. A. Lobach, and S. I. Kablukov, "Application of a self-sweeping Yb-doped fiber laser for high-resolution characterization of phase-shifted FBGs," *J. Lightwave Technol.*, vol. 31, no. 18, p. 2982-2987, Sept. 2013.

[22] Xiong Wang, Pu Zhou, Xiaolin Wang, Hu Xiao, and Lei Si, "Tm-Ho co-doped all-fiber brand-range self-sweeping laser around 1.9 μm," *Opt. Express*, vol. 21, no. 14, pp. 16290-16295, July 2013.

[23] I. A. Lobach, S. I. Kablukov, M. A. Melkumov, V. F. Khopin, S. A. Babin, and E. M. Dianov, "Single-frequency Bismuth-doped fiber laser with quasi-continuous self-sweeping," *Opt. Express*, vol. 23, no. 19, pp. 24833-24842, Sept. 2015.

[24] J. Aubrecht, P. Peterka, P. Honzatko, P. Koska, O. Podrazky, F. Todorov, and I. Kasik, "Self-swept holmium fiber laser near 2100 nm," *Opt. Express*, vol. 25, no. 4, 4120-4125, Feb. 2017.

[25] S. Sugavanam, S. Fabbri, S. T. Le, I. Lobach, S. Kablukov, S. Khorev, and D. Churkin, "Real-time high-resolution heterodyne-based measurements of spectral dynamics in fibre lasers," *Sci. Rep.*, vol. 6, p. 23152, March 2016.

[26] P. Peterka, P. Honzátko, J. Aubrecht, P. Navrátil, P. Koška, F. Todorov, O. Podrazký, J. Čtyroký, I. Kašík, "Self-sweeping of laser wavelength and associated mode instabilities in fiber lasers," In *Proc. 19th Int. Conf. on Transparent Optical Networks (ICTON)*, Girona, Catalonia, Spain, 2-6 July 2017, p. Tu.B6.2.

[27] A. A. Fotiadi, O. L. Antipov and P. Mégret, "Resonantly induced refractive index changes in Yb-doped fibers: the origin, properties and application for all-fiber coherent beam combining," in *Frontiers in guided wave optics and optoelectronics*, Bishnu Pal (Ed.), InTech, 2010.

[28] M. J. F. Digonnet, R. W. Sadowski, H. J. Shaw, and R. H. Pantell, "Experimental evidence for the strong UV transition contribution in the resonant nonlinearity of doped fibers," *J. Lightwave Technol.*, vol. 15, no. 2, pp. 299–303, Feb. 1997.

[29] J. W. Arkwright, P. Elango, G. R. Atkins, T. Whitbread, and J. F. Digonnet, "Experimental and theoretical analysis of the resonant nonlinearity in ytterbium-doped fiber," *J. Lightwave Technol.*, vol. 16, no. 5, pp. 798–806, May 1998.

[30] K. O. Hill, Y. Fujii, D. C. Johnson, and B. S. Kawasaki, "Photosensitivity in optical fiber waveguides: Application to reflection filter fabrication," *Appl. Phys. Lett.*, vol. 32, no. 10, pp. 647-649, May 1978.

[31] P. Peterka, P. Honzatko, F. Todorov, J. Aubrecht, O. Podrazky, and I. Kasik, "Self-Q-switched regime of fiber lasers as a transition from self-induced laser line sweeping," in *OSA Technical Digest Advanced Photonics*, Barcelona, Spain, 27–31 July 2014, p. SoTh2B.6.

[32] P. Peterka, P. Honzatko, P. Koska, F. Todorov, J. Aubrecht, O. Podrazky, and I. Kasik, "Reflectivity of transient Bragg reflection gratings in fiber laser with laser-wavelength self-sweeping," *Opt. Express*, vol. 22, no. 24, pp. 30024-30031, Dec. 2014.

[33] P. Peterka, P. Honzatko, P. Koska, F. Todorov, J. Aubrecht, O. Podrazky, and I. Kasik, "Reflectivity of transient Bragg reflection gratings in fiber laser with laser-wavelength self-sweeping: erratum," *Opt. Express*, vol. 24, no. 14, pp. 16222-16223, July 2016.

[34] A. Lobach, R. V. Drobyshev, A. A. Fotiadi, S. I. Kablukov, and S. A. Babin, "The reflectivity measurement of a dynamically formed fiber Bragg grating inside an Yb-doped fiber," in *OSA Technical Digest Frontiers in Optics*, Rochester, USA, 17-21 Oct. 2016, p. FTu2I.6.

[35] P. Peterka, B. Faure, W. Blanc, M. Karasek, and B. Dussardier, "Theoretical modelling of S-band thulium-doped silica fibre amplifiers," *Opt. Quant. Electron.*, vol. 36, no. 1-3, pp. 201-212, Jan. 2004.

[36] P. Peterka, I. Kasik, A. Dhar, B. Dussardier, and W. Blanc, "Theoretical modeling of fiber laser at 810 nm based on thulium-doped silica fibers with enhanced $^3H_4$ level lifetime," *Opt. Express*, vol. 19, no. 3, pp. 2773-2781, Jan. 2011.

[37] Dietrich Marcuse, *Theory of dielectric optical waveguides*. Academic Press, New York and London 1974.

[38] H. Kogelnik, "Filter response of nonuniform almost-periodic structures," *Bell Sys. Tech. J.*, vol. 55, no. 1, pp. 109-126, Jan 1976.

[39] H. Kogelnik, "Theory of optical waveguides," in *Guided-Wave Optoelectronics*. T. Tamir, Ed., New York: Springer-Verlag, 1990.

[40] A. Othonos and K. Kalli, *Fiber Bragg gratings: fundamentals and applications in telecommunications and sensing*. Artech House, 1999, pp. 189-193.

[41] R. Kashyap, *Fiber Bragg Gratings*. 2nd edition, Academic Press, Elsevier, 2009.

[42] T. Erdogan, "Fiber grating spectra," *J. Lightwave Technol.*, vol. 15, no. 8, pp. 1277–1294, Aug. 1997.

[43] E. Desurvire, *Erbium-Doped Fiber Amplifiers, Principles and Applications*, John Wiley & Sons, New York, 1994.

[44] P. Peterka and J. Kanka, "Erbium-doped twin-core fibre narrow-band filter for fibre lasers," *Opt. Quant. Electron.*, vol. 33, no. 4-5, pp. 571-581, Apr. 2001.

[45] I. A. Lobach, R. V. Drobyshev, A. A. Fotiadi, E. V. Podivilov, S. I. Kablukov, and S. A. Babin, "Open-cavity fiber laser with distributed feedback based on externally or self-induced dynamic gratings," *Opt. Lett.*, vol. 42, no. 20, pp. 4207-4210, Oct. 2017.

https://doi.org/10.1109/JSTQE.2018.2806084

Pavel Peterka received his MSc degree in physical engineering in 1993 and PhD degree in radioelectronics in 2000 from the Czech Technical University in Prague. Within 2001-3 he worked 13 months in Laboratoire de Physique de la Matière Condensée (LPMC), CNRS - Université de Nice – Sophia Antipolis, Nice in France on thulium-doped fibers. He is currently a senior research scientist at the Institute of Photonics and Electronics of the Czech Academy of Sciences. His research interests cover numerical modeling and spectroscopic characterization of rare-earth-doped fibers, development of specialty fibers and components for fiber lasers. Since 2007, he has been teaching a one-semester course on fiber lasers and amplifiers at the Czech Technical University.

Pavel Koška received the MSc degree in physical engineering in 2008 and MSc degree in electrical engineering in 2014; both from the Czech Technical University. He defended his PhD thesis "Linear and nonlinear optical fiber microstructures finite element modeling" in 2016 while working at the Institute of Photonics and Electronics of the Czech Academy of Sciences. His research interest is numerical analysis and design of photonic and microelectronic devices.

Jiří Čtyroký (M'90–SM'99) received the Ing. (M.S.) degree in microwave engineering and the C.Sc. (Ph.D.) degree in applied physics from the Faculty of Electrical Engineering, Czech Technical University, Prague, Czech Republic, in 1968 and 1972, respectively, and the Dr.Sc. degree in electronics from the Academy of Sciences of the Czech Republic, Prague, in 1990. Since 1973, he has been a Research Scientist with the Institute of Radio Engineering and Electronics (now the Institute of Photonics and Electronics AS CR, v.v.i.), Prague. As a Professor of applied physics, he is also active as a teacher of guided electromagnetic waves, integrated photonics and optoelectronics at the Czech Technical University, Prague. His current interests include all aspects of guided-wave photonics. In this field, he authored and co-authored more than 100 papers and conference contributions. J. Čtyroký is a member of the Optical Society of America, the Institute of Physics (FInstP and CPhys), EOS, and the Czech and Slovak Society for Photonics.